Nucl Med Mol Imaging (2012) 46:254–260
DOI 10.1007/s13139-012-0159-3

ORIGINAL ARTICLE

Validation of Simple Quantification Methods for ^{18}F-FP-CIT PET Using Automatic Delineation of Volumes of Interest Based on Statistical Probabilistic Anatomical Mapping and Isocontour Margin Setting

Yong-il Kim · Hyung-Jun Im · Jin Chul Paeng · Jae Sung Lee · Jae Seon Eo · Dong Hyun Kim · Euishin E. Kim · Keon Wook Kang · June-Key Chung · Dong Soo Lee

Received: 28 March 2012 / Revised: 18 June 2012 / Accepted: 9 July 2012 / Published online: 2 August 2012

Abstract
Purpose ^{18}F-FP-CIT positron emission tomography (PET) is an effective imaging for dopamine transporters. In usual clinical practice, ^{18}F-FP-CIT PET is analyzed visually or quantified using manual delineation of a volume of interest (VOI) for the striatum. In this study, we suggested and validated two simple quantitative methods based on automatic VOI delineation using statistical probabilistic anatomical mapping (SPAM) and isocontour margin setting.
Methods Seventy-five ^{18}F-FP-CIT PET images acquired in routine clinical practice were used for this study. A study-specific image template was made and the subject images were normalized to the template. Afterwards, uptakes in the striatal regions and cerebellum were quantified using probabilistic VOI based on SPAM. A quantitative parameter, Q_{SPAM}, was calculated to simulate binding potential. Additionally, the functional volume of each striatal region and its uptake were measured in automatically delineated VOI using isocontour margin setting. Uptake-volume product (Q_{UVP}) was calculated for each striatal region. Q_{SPAM} and Q_{UVP} were compared with visual grading and the influence of cerebral atrophy on the measurements was tested.
Results Image analyses were successful in all the cases. Both the Q_{SPAM} and Q_{UVP} were significantly different according to visual grading ($P<0.001$). The agreements of Q_{UVP} or Q_{SPAM} with visual grading were slight to fair for the caudate nucleus ($\kappa=0.421$ and 0.291, respectively) and good to perfect to the putamen ($\kappa=0.663$ and 0.607, respectively). Also, Q_{SPAM} and Q_{UVP} had a significant correlation with each other ($P<0.001$). Cerebral atrophy made a significant difference in Q_{SPAM} and Q_{UVP} of the caudate nuclei regions with decreased ^{18}F-FP-CIT uptake.
Conclusion Simple quantitative measurements of Q_{SPAM} and Q_{UVP} showed acceptable agreement with visual grading. Although Q_{SPAM} in some group may be influenced by cerebral atrophy, these simple methods are expected to be effective in the quantitative analysis of ^{18}F-FP-CIT PET in usual clinical practice.

Keywords ^{18}F-FP-CIT PET · PET · Statistical probabilistic anatomical mapping · Volume of interest · Validation

Y.-i. Kim · H.-J. Im · J. C. Paeng (✉) · J. S. Lee (✉) · J. S. Eo · K. W. Kang · J.-K. Chung · D. S. Lee
Department of Nuclear Medicine,
Seoul National University Hospital,
101 Daehak-ro, Jongno-gu,
Seoul 110-744, South Korea
e-mail: paengjc@snu.ac.kr
e-mail: jaes@snu.ac.kr

Y.-i. Kim · H.-J. Im · E. E. Kim · D. S. Lee
Department of Molecular Medicine and Biopharmaceutical Sciences, WCU Graduate School of Convergence Science and Technology, Seoul National University,
Seoul, South Korea

D. H. Kim
Department of Radiology, Seoul National University Hospital,
Seoul, South Korea

E. E. Kim
Department of Nuclear Medicine, MD Anderson Cancer Center,
Houston, TX, USA

Introduction

Parkinson's disease is a progressive neurodegenerative disorder of nigrostriatal dopaminergic neurons [1]. Nuclear imaging methods for the dopaminergic system using SPECT or PET are reliable and objective diagnostic tools for

Parkinson's syndromes. Among diverse radiopharmaceuticals for dopaminergic system, tropane derivatives, ^{123}I-FP-CIT or ^{123}I-beta-CIT, have been used to evaluate the dopamine transporters successfully [2–4]. Currently, ^{18}F-FP-CIT positron emission tomography (PET) is widely used in assessing the dopaminergic transporter [5, 6], with a governmental drug approval in Korea. ^{18}F-FP-CIT has fast kinetics and can provide images with high signal-to-noise ratio [7].

In the analysis of ^{18}F-FP-CIT PET in usual clinical practice, visual assessment with semi-quantitative grading is commonly performed [8, 9]. For more close interpretation with quantitative analysis, delineation of volumes of interest (VOI) is required to measure uptake of ^{18}F-FP-CIT in the striatum and reference regions. A VOI can be drawn manually with aid of magnetic resonance imaging (MRI) or semi-automatically using standard VOI [10–12]. Another method for VOI delineation is normalization of image to a standard brain template [13–15]. However, these methods are still laborious for routine clinical practice.

Statistical probabilistic anatomical mapping (SPAM) is a mapping method for specific brain structures, providing a probability to be a specific structure for each voxel. In spatially normalized brain images, SPAM can provide probabilistic VOI with high accuracy, reproducibility, and ease. Particularly in Korea, a Korean standard template for SPAM has been developed [16] and used in many studies on brain perfusion single-photon emission tomography (SPECT) and ^{18}F-FDG PET. Also for dopamine transporter imaging, the SPAM method was applied for analysis of ^{123}I-CIT SPECT previously [17]. Application of SPAM to image analysis is very simple and objective.

Additionally, another simple VOI delineation method is available by isocontour margin setting. Currently, most image analysis software packages provide automatic VOI by simple setting of a margin threshold, as a standardized uptake value (SUV) or a percentage of maximal uptake. In the analysis of ^{18}F-FDG PET, metabolic tumor volume and total-lesion glycolysis can be measured with these software packages. As a simplified method for delineation of functional volume, we adopted this method to calculate functional volume and uptake-volume product. This may be a surrogate marker for total amount of the functional dopamine transporters.

In this study, we applied a SPAM method for analysis of ^{18}F-FP-CIT PET, and tried to validate it. Also, we tried to validate the method of automatic VOI delineation based on isocontour margin setting.

Materials and Methods

Subjects and Image Acquisition

^{18}F-FP-CIT PET images of 75 patients (males/females=35/40, age 59.2±14.4 years, range 19–81 years) that were consecutively acquired from June 2009 to Dec 2009 were retrospectively included in this study. All the patients had clinical symptoms suggesting Parkinson's disease and the PET images were performed in routine clinical practice. All the ^{18}F-FP-CIT PET images were acquired using a dedicated PET/computed tomography (CT) scanner equipped with a 40-slice CT scanner (Biograph40, Siemens Healthcare). Patients were injected with ^{18}F-FP-CIT (185 MBq) and images were acquired 2 h after injection. Brain PET image was acquired for 10 min following CT scan for attenuation correction. PET image was reconstructed with an iterative algorithm (ordered subset expectation maximization) with image size of 256×256 matrix. On 75 PET scans, 300 regions of striatum were visually graded. Among 150 bilateral striatal regions, 69 (46 %) caudate nuclei and 112 (75 %) putamina showed abnormal uptake (Table 1). MRI images were acquired within 149±31 days from ^{18}F-FP-CIT PET using field strengths of 1.0-T (Magnetom Expert; Siemens) or 1.5-T (Signa, GE Healthcare, or Magnetom Vision Plus, Siemens) with a standard quadrature head coil. T2-weighted and fluid attenuation inversion recovery (FLAIR) sequence MR images were used for review. MRI was acquired in 74 patients, with missing in one patient. MRI demonstrated no or mild atrophy in 43 patients, moderate to severe atrophy in 31 patients.

Visual Analysis of ^{18}F-FP-CIT PET and MRI

Two nuclear medicine physicians visually analyzed ^{18}F-FP-CIT PET images and graded uptake of ^{18}F-FP-CIT for four regions of the striatum (both caudate nuclei and putamina) by consensus. Each region was graded using a three-grade system (normal, mild to moderate, and severe decrease in uptake). Examples of the grading are shown in Fig. 1. In addition, we assumed that brain atrophy status may induce variability in the anatomical structure of the brain including striatum, and may affect the automatic process of ^{18}F-FP-CIT PET quantification [21]. To analyze the effect of cerebral atrophy on the SPAM-based automatic VOI delineation, cerebral atrophy was also graded on MRI using a two-grade system (no or mild atrophy, and moderate to severe atrophy,

Table 1 Number of striatal regions in each group of visual grading

	Uptake decrease		
	Normal	Mild to moderate	Severe
R caudate	41	28	6
L caudate	40	30	5
R putamen	19	32	24
L putamen	19	26	30

R right, *L* left

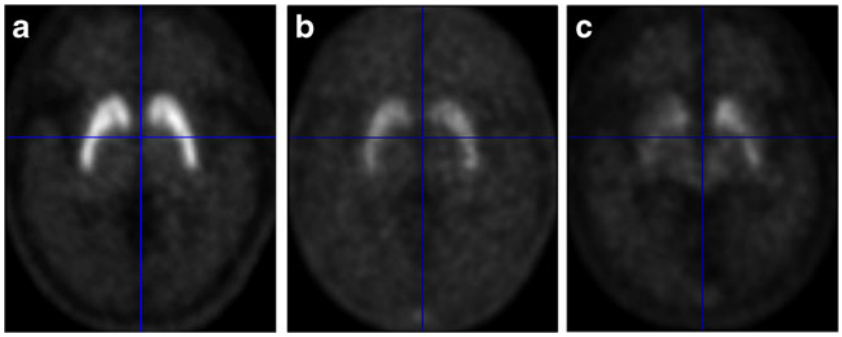

Fig. 1 Examples of visual grading for ^{18}F-FP-CIT PET; normal (**a**), mild to moderate decrease (**b**), and severe decrease in uptake (**c**)

according to the brain parenchyme shrinkage, flattening of brain cortical convexity, and widening of sulci and ventricles) by consensus of two nuclear medicine physicians.

SPAM-Based Automatic VOI and Quantification

A study-specific template was created using the same procedure employed in our previous study for ^{123}I-beta-CIT SPECT [16]. Briefly, an initial template was generated by summing the SPAM images [15] of striatum, brain, and head, with multiplying different weighting factors (9.0, 0.5, and 0.5, respectively). Afterward, the initial template was smoothed with a 12-mm Gaussian kernel to adjust resolution. The final study-specific template was obtained by averaging all the subjects' PET images that were spatially normalized to the initial template (Fig. 2). Entire process of image manipulation was performed using SPM99 (University College of London, UK) implemented on Matlab 6.5 (The Mathworks, Natick, MA, USA).

^{18}F-FP-CIT PET images of the subjects were normalized to the study-specific template using SPM2, without additional smoothing. On normalized ^{18}F-FP-CIT PET images, uptake of ^{18}F-FP-CIT in the four regions of the striatum and cerebellum were calculated based on the anatomical map of a Korean SPAM [16]; count and anatomical probability of each voxel were multiplied and summed for each region. A quantification value of uptake in the VOI was defined as Q_{SPAM}=[(striatum value)−(cerebellum value)]/(cerebellum value), to simulate the binding potential. The reproducibility of this method was 100 % without variation according to operators.

Threshold-Based Automatic VOI and Quantification

For threshold-based automatic VOI, PET images were analyzed using a vendor-supplied viewing and analysis software package, syngo.via (Siemens Healthcare, Forchheim, Germany). An elliptical VOI was drawn to include each of four striatum regions. Afterward, a target VOI was automatically drawn in the elliptical VOI by the software with setting a threshold for isocontour margin. We applied a margin threshold of SUV 2.5, based on our pilot study in which normal cerebellum demonstrated maximum SUV of 2.33±0.75 (range, 1.73–2.74). Mean uptake (mean SUV) and volume (cm^3) were measured for the target VOI, and a quantification value of uptake-volume product was defined as Q_{UVP}=(mean SUV)×(volume).

Statistical Analysis

Statistical analyses were performed separately for the caudate nucleus and putamen. Results were expressed as mean ± SD. Comparison between visual analysis and automatic

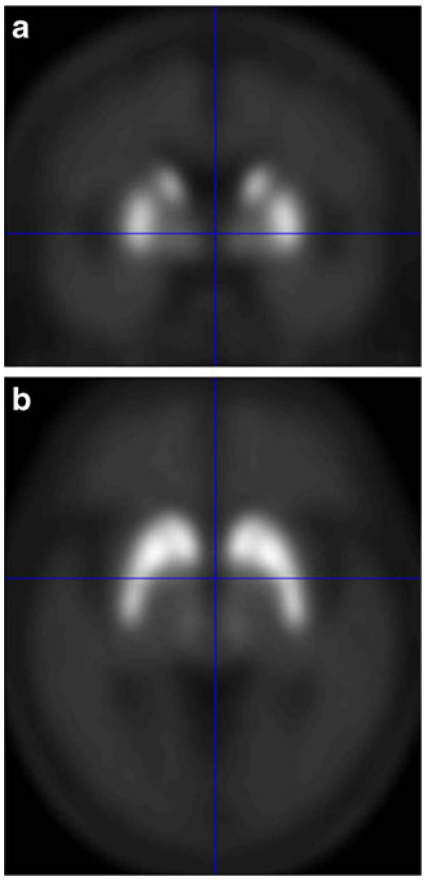

Fig. 2 Study-specific template of^{18}F-FP-CIT PET, which was made by averaging all the patients' ^{18}F-FP-CIT PET images; coronal (**a**) and transaxial (**b**) views

VOI methods were performed by one-way analysis of variance (ANOVA). To evaluate inter-modality agreement, Cohen's κ values were calculated; each region was re-graded into three grades based on values of Q_{SPAM} or Q_{UVP}, and weighted κ values were calculated. In this analysis, grading cutoff was acquired from receiver-operating characteristics (ROC) curve analyses. Influence of cerebral atrophy on the quantification was evaluated by Student's *t*-test in each visual grade group. Correlations between values were tested by Pearson's correlation analysis. The statistical analyses were performed by a software package of SPSS 18.0 (IBM, Chicago, IL, USA) and MedCalc (MedCalc, Mariakerke, Belgium).

Results

Comparison of Q_{SPAM}, Q_{UVP} and Visual Grading

Normalization of the PET images and calculation of Q_{SPAM} was successfully performed with all of the 75 PET scans. In both the caudate nucleus and putamen, Q_{SPAM} was significantly decreased according to severity of visual grades ($P<0.001$, Fig. 3).

Uptake of the caudate nucleus was re-graded into a three-grade system by Q_{SPAM}, with cutoff values of 3.10 and 2.14, respectively, which were determined in ROC analyses. The κ value for agreement between visual and Q_{SPAM} grading was 0.421, which means fair agreement. Similarly, uptake of the putamen was re-graded with cutoff Q_{SPAM} values of 3.74 and 3.00, respectively, and the κ value for agreement between visual and Q_{SPAM} grading was 0.607, which means good to perfect agreement.

In both the caudate nucleus and putamen, Q_{UVP} was also significantly decreased according to severity of visual grading ($P<0.001$, Fig. 4). Uptake of the caudate nucleus was re-graded into a three-grade system by Q_{UVP}, with cutoff values of 10.06 and 7.44, respectively. The κ value for agreement between visual and Q_{UVP} grading was 0.291, which means slight agreement. However, when uptake of the putamen was re-graded with cutoff Q_{UVP} values of 19.31 and 6.63, respectively, the κ value for agreement between visual and Q_{SPAM} grading was 0.663, which means good to perfect agreement.

Q_{SPAM} and Q_{UVP} had a significant correlation with each other in both the caudate nucleus and putamen (Fig. 5). Pearson's correlation coefficients were 0.634 in the caudate nucleus ($P<0.001$) and 0.765 in the putamen, respectively ($P<0.001$).

Effect of Cerebral Atrophy on Quantification

In each visual grade group, Q_{SPAM} and Q_{UVP} were compared between groups with different cerebral atrophy. The caudate nuclei with normal uptake in visual grading demonstrated no difference of Q_{SPAM} according to cerebral atrophy (Table 2). However, in the caudate nuclei with mild to moderate uptake decrease, the group with severer cerebral atrophy demonstrated significantly lower Q_{SPAM}. In the caudate nuclei with severe uptake decrease, Q_{SPAM} was lower in the group with severer cerebral atrophy, although statistical significance was not calculated due to small sample size. Also, Q_{UVP} showed similar difference according to cerebral atrophy in the caudate nuclei. In contrast, no significant influence of cerebral atrophy on Q_{SPAM} and Q_{UVP} existed in any of visual grade groups in the putamen (Table 2).

Discussion

In the current study, we evaluated the validity of two simple automatic VOI delineation methods for analysis of ^{18}F-FP-CIT PET. As a result, Q_{SPAM} and Q_{UVP}, which are based on SPAM and automatic VOI delineation with isocontour margin setting, respectively, showed satisfactory agreement

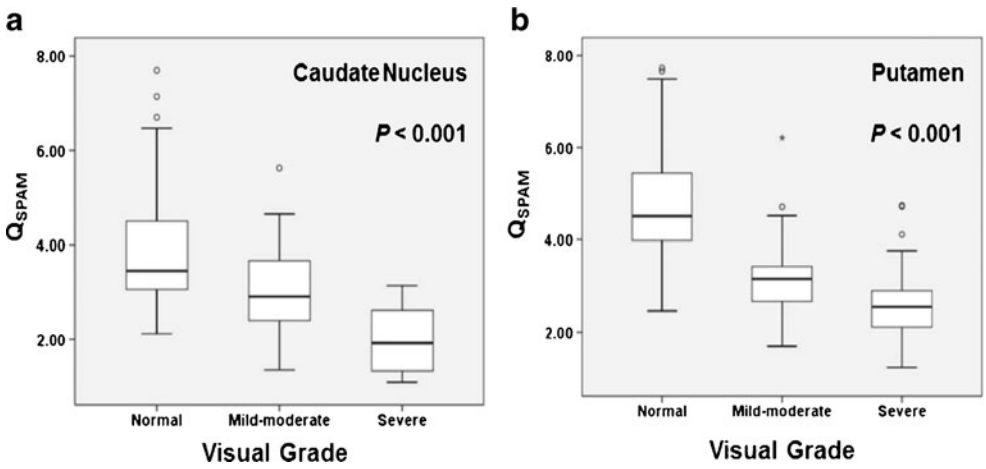

Fig. 3 Distribution of Q_{SPAM} according to visual grade group. Both the caudate nucleus (**a**) and putamen (**b**) showed significant difference of Q_{SPAM} according to visual grade groups ($P<0.001$, respectively)

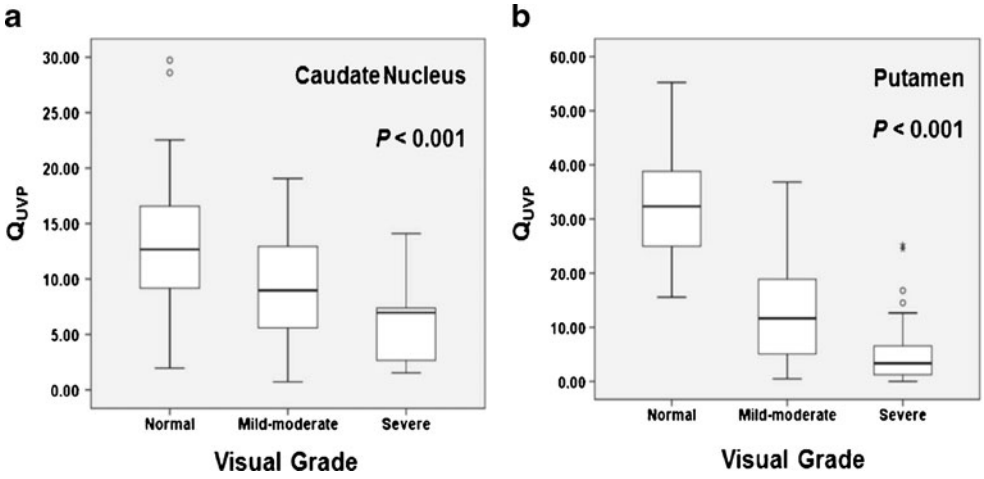

Fig. 4 Distribution of Q_{UVP} according to visual grade group. Both the caudate nucleus (**a**) and putamen (**b**) showed significant difference of Q_{UVP} according to visual grade groups ($P<0.001$, respectively)

with visual grading. Additionally, they had good correlation with each other.

^{18}F-FP-CIT PET is an effective imaging for diagnostic evaluation of Parkinson's syndrome by visualizing dopamine transporters [14]. In current clinical practice, the usual analysis method for ^{18}F-FP-CIT PET is visual qualitative assessment or quantitative measurement of binding potential using manual VOI delineation [18]. More complicated methods such as PET-MRI fusion may be used for accurate VOI delineation; however, these methods have poor availability in routine clinical practice currently. Although visual assessment or manual VOI delineation by experts are practical and effective analysis tools, they are operator-dependent and lack objectivity and reproducibility.

For regional analysis of brain images, SPAM has been developed for normalized brain image templates. In Korea, SPAM was developed for Korean standard brain image templates [16], following that of the International Consortium for Brain Mapping [19]. Once spatial normalization of an individual image is successful, image parameters of target VOIs, predefined structures on a standard template can simply be measured automatically. Thus, SPAM can provide objective regional analysis of functional brain images, with ease and near-complete reproducibility [20].

Based on SPAM, we developed a simple analysis method for ^{18}F-FP-CIT PET [17], and validated it in the current study. The SPAM-based VOI delineation was successfully performed in all the 75 subjects and the measurement of Q_{SPAM} had a perfect reproducibility. In agreement analysis, Q_{SPAM} had fair to perfect agreement with visual grading, particularly for the putamen that is a much more vulnerable region in Parkinson's disease. Thus, Q_{SPAM} analysis may be used in clinical practice at least to assist visual analysis. Further validation is required to be used in more precise analysis; however, currently no absolute reference method exists for accurate VOI delineation of striatal structures. A hybrid PET/MRI scanner may be a solution for further validation, as well as PET-MRI coregistration analysis.

Koch et al. [21] reported that cerebral atrophy may affect automatic and observer-independent evaluation of dopamine transporter SPECT, probably due to normalization errors. When brain atrophy is severe, normalization to a template may have some error due to anatomical variations of the brain structures, including basal ganglia. Additionally,

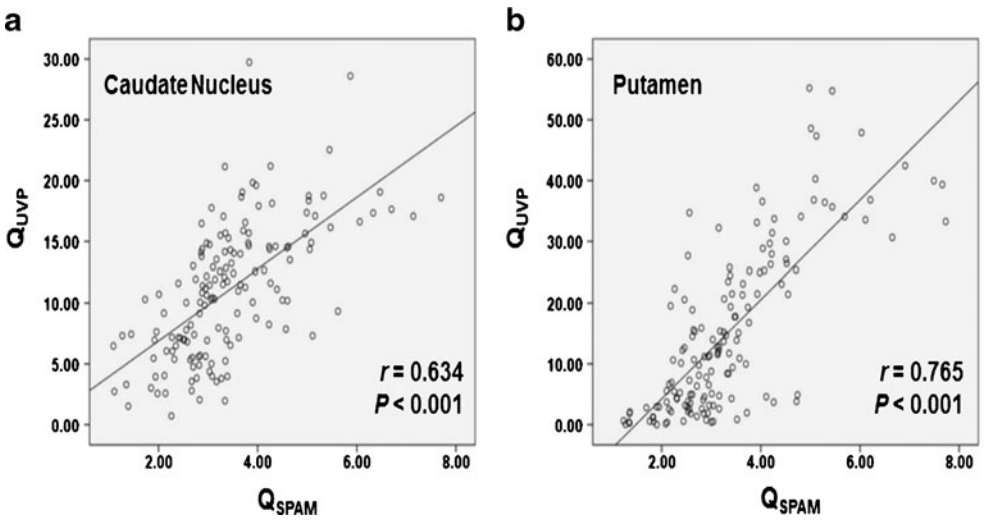

Fig. 5 Correlation analysis between Q_{SPAM} and Q_{UVP}. Both the caudate nucleus (**a**) and putamen (**b**) showed significant correlation between Q_{SPAM} and Q_{UVP}

Table 2 Influence of cerebral atrophy on measurement of Q_{SPAM}

	Q_{SPAM}			Q_{UVP}		
Visual grading of ^{18}F-FP-CIT uptake	Normal or mild atrophy	Moderate to severe atrophy	*P*	Normal or mild atrophy	Moderate to severe atrophy	*P*
Caudate						
0	3.95±1.26	3.56±0.76	0.105	12.76±5.45	12.13±4.39	0.631
1	3.43±0.90	2.68±0.67	0.001	11.45±4.55	7.34±3.53	0.000
2	2.83[a]	1.88±0.74	NA[a]	2.05[*]	6.82±3.98	NA[a]
Putamen						
0	4.90±1.44	4.30±0.89	0.151	32.45±10.07	30.02±7.23	0.509
1	3.05±0.72	3.10±0.56	0.746	11.65±8.16	13.84±9.03	0.343
2	2.64±0.72	2.47±0.85	0.432	4.81±4.07	5.47±7.33	0.677

[a] SD and *P* values were not calculated due to existence of only one sample in a group

when cerebral glucose metabolism in normal aging was investigated using automatic VOI delineation by SPAM, regional heterogeneity was increased with aging [22], which may also be caused by cerebral atrophy in the aged brain. In the current study, Q_{SPAM} and Q_{UVP} were significantly different according to cerebral atrophy in the groups with decreased uptake in visual analysis, whereas no significant difference existed in the visually normal group. The difference may have been caused by real pathophysiological difference, as brain atrophy is a major sign for cerebral degeneration. The variation of measurements expressed in the coefficient of variation was lower in the groups with cerebral atrophy. Additionally, another quantified value of Q_{UVP} that did not undergo image processing also showed a similar result. However, the difference between the caudate and putamen suggests influence of methodological factor, as the structure of the putamen is more simple than that of the caudate. It should be investigated in further studies whether the difference was caused by the SPAM method with image normalization, or pathophysiological correlation between atrophy and dopamine transporter.

Q_{UVP} is based on a simple VOI delineation method that is currently equipped in many commercial image analysis software packages. When a VOI is determined by a specific threshold on a functional PET image, it would reflect a volume of functional tissue. Likewise, uptake-volume product would reflect total amount of functional activity. Measurements of metabolic tumor volume and total-lesion glycolysis on ^{18}F-FDG PET are based on this concept. In the current study, Q_{UVP} demonstrated no less agreement with visual grading than that of Q_{SPAM} for the putamen, although it did not for the caudate nucleus. However, Q_{UVP} is very simple to measured and has a great potential for routine clinical practice.

Although the current study demonstrated the potential of two simple methods for quantification of ^{18}F-FP-CIT PET, the methods require further refinement. Our image template for image normalization and SPAM was acquired by averaging all the subjects' images in this study (the study-specific template). In our previous study, the study-specific template showed better results than a preformed template in the analysis. To make optimal templates that may be institute-specific or population-specific, further research is required for the necessary number of images, inclusion criteria, and so forth. Also for measurement of Q_{UVP}, methods to determine optimal threshold should be investigated. In the current study, we adopted a crude cutoff of SUV 2.5, based on average maximal uptake of the cerebellum that is used as a reference region. This study was a kind of proof-of-concept study for application of the methods, and further studies are required for the optimal or individualized cutoff threshold, probably individualized one.

This study has a limitation that it validated Q_{SPAM} or Q_{UVP} with reference of visual grading because Q_{SPAM} or Q_{UVP} was regarded as a complementary parameter to visual analysis in clinical practice. However, in further studies, it is required that Q_{SPAM} and Q_{UVP} be validated with reference of more precise quantitative values. Hybrid PET/MRI-based quantification may be an optimal reference method. Additionally, the clinical efficacy of these parameters should be investigated with regard to clinical severity of Parkinson's disease.

Conclusions

Simple quantitative measurements of Q_{SPAM} and Q_{UVP}, based on VOI delineation using SPAM and isocontour margin setting, respectively, showed acceptable agreement with visual grading in the analysis of ^{18}F-FP-CIT PET. Additionally, they had significant correlation with each other. Thus, these simple methods would be effective in the quantitative

analysis of ^{18}F-FP-CIT PET in usual clinical practice as supplementary methods. Further studies are required to investigate the clinical efficacy of these measurements and to refine the methods, particularly regarding image template for Q_{SPAM} and the optimal threshold setting for Q_{UVP}.

Acknowledgments This work was supported by the National Research Foundation of Korea (NRF) grant funded by the Korean government (MEST) (no. 2011K000719)

Conflicts of Interest None.

References

1. Niznik HB, Fogel EF, Fassos FF, Seeman P. The dopamine transporter is absent in parkinsonian putamen and reduced in the caudate nucleus. J Neurochem. 1991;56:192–8.
2. Klaffke S, Kuhn AA, Plotkin M, Amthauer H, Harnack D, Felix R, et al. Dopamine transporters, D2 receptors, and glucose metabolism in corticobasal degeneration. Mov Disord. 2006;21:1724–7.
3. Kas A, Payoux P, Habert MO, Malek Z, Cointepas Y, El Fakhri G, et al. Validation of a standardized normalization template for statistical parametric mapping analysis of ^{123}I-FP-CIT images. J Nucl Med. 2007;48:1459–67.
4. Oh SW, Kim YK, Lee BC, Kim BS, Kim JS, Kim JM, et al. Evaluation of multiple system atrophy and early Parkinson's disease using ^{123}I-FP-CIT SPECT. Nucl Med Mol Imaging. 2009; 43:10–8.
5. Kazumata K, Dhawan V, Chaly T, Antonini A, Margouleff C, Belakhlef A, et al. Dopamine transporter imaging with fluorine-18-FPCIT and PET. J Nucl Med. 1998;39:1521–30.
6. Oh JK, Yoo ID, Seo YY, Chung YA, Yoo IR, Kim SH, et al. Clinical significance of F-18 FP-CIT dual time point PET imaging in idiopathic Parkinson's disease. Nucl Med Mol Imaging. 2011; 45:255–60.
7. Robeson W, Dhawan V, Belakhlef A, Ma Y, Pillai V, Chaly T, et al. Dosimetry of the dopamine transporter radioligand ^{18}F-FPCIT in human subjects. J Nucl Med. 2003;44:961–6.
8. O'Brien JT, McKeith IG, Walker Z, Tatsch K, Booij J, Darcourt J, et al. Diagnostic accuracy of ^{123}I-FP-CIT SPECT in possible dementia with Lewy bodies. Br J Psychiatr. 2009;194:34–9.
9. Marshall VL, Reininger CB, Marquardt M, Patterson J, Hadley DM, Oertel WH, et al. Parkinson's disease is overdiagnosed clinically at baseline in diagnostically uncertain cases: a 3-year European multicenter study with repeat [^{123}I]FP-CIT SPECT. Mov Disord. 2009;24:500–8.
10. Eggers C, Kahraman D, Fink GR, Schmidt M, Timmermann L. Akinetic–rigid and tremor–dominant Parkinson's disease patients show different patterns of FP-CIT single photon emission computed tomography. Mov Disord. 2011;26:416–23.
11. Oh M, Kim JS, Kim JY, Shin KH, Park SH, Kim HO, et al. Subregional patterns of preferential striatal dopamine transporter loss differ in Parkinson disease, progressive supranuclear palsy, and multiple-system atrophy. J Nucl Med. 2012;53:399–406.
12. Contrafatto D, Mostile G, Nicoletti A, Dibilio V, Raciti L, Lanzafame S, et al. [^{123}I] FP-CIT SPECT asymmetry index to differentiate Parkinson's disease from vascular parkinsonism. Acta Neurol Scand. 2012;126:12-6
13. Ma Y, Dhawan V, Mentis M, Chaly T, Spetsieris P, Eidelberg D. Parametric mapping of [^{18}F]FPCIT binding in early stage Parkinson's disease: a PET study. Synapse. 2002;45:125–33.
14. Wang J, Zuo CT, Jiang YP, Guan YH, Chen ZP, Xiang JD, et al. ^{18}F-FP-CIT PET imaging and SPM analysis of dopamine transporters in Parkinson's disease in various Hoehn & Yahr stages. J Neurol. 2007;254:185–90.
15. Eshuis S, Jager P, Maguire R, Jonkman S, Dierckx R, Leenders K. Direct comparison of FP-CIT SPECT and F-DOPA PET in patients with Parkinson's disease and healthy controls. Eur J Nucl Med Mol Imaging. 2009;36:454–62.
16. Lee JS, Lee DS, Kim YK, Kim JS, Lee JM, Koo BB, et al. Quantification of brain images using korean standard templates and structural and cytoarchitectonic probabilistic maps. Korea J Nucl Med. 2004;38:241–52.
17. Eo JS, Lee H-Y, Lee JS, Kim YK, Jeon B-S, Lee DS. Automated analysis of ^{123}I-beta-CIT SPECT images with statistical probabilistic anatomical map. MS Thesis. Seoul: Seoul National University 2006.
18. Colloby SJ, O'Brien JT, Fenwick JD, Firbank MJ, Burn DJ, McKeith IG, et al. The application of statistical parametric mapping to ^{123}I-FP-CIT SPECT in dementia with Lewy bodies, Alzheimer's disease and Parkinson's disease. NeuroImage. 2004;23: 956–66.
19. Mazziotta J, Toga A, Evans A, Fox P, Lancaster J, Zilles K, et al. A probabilistic atlas and reference system for the human brain: International Consortium for Brain Mapping (ICBM). Philos Trans R Soc B. 2001;356:1293–322.
20. Lee JS, Lee DS. Analysis of functional brain images using population-based probabilistic atlas. Curr Med Imaging Rev. 2005;1:81–7.
21. Koch W, Radau PE, Hamann C, Tatsch K. Clinical testing of an optimized software solution for an automated, observer-independent evaluation of dopamine transporter SPECT studies. J Nucl Med. 2005;46:1109–18.
22. Lee JS, Lee DS, Park KS, Chung JK, Lee MC. Changes in the heterogeneity of cerebral glucose metabolism with healthy aging: quantitative assessment by fractal analysis. J Neuroimaging. 2004;14:350–6.